Title
Hemodynamics and Ventricular Function in a Zebrafish Model of Injury and Repair

Journal
Zebrafish, 11(5)

ISSN
1545-8547

Authors
Lee, Juhyun
Cao, Hung
Kang, Bong Jin
et al.

Publication Date
2014-10-01

DOI
10.1089/zeb.2014.1016

Peer reviewed

ZEBRAFISH
Volume 11, Number 5, 2014

DOI: 10.1089/zeb.2014.1016

Hemodynamics and Ventricular Function in a Zebrafish Model of Injury and Repair

Juhyun Lee,[1,2,*] Hung Cao,[1,*] Bong Jin Kang,[3,*] Nelson Jen,[2,*] Fei Yu,[3] Chia-An Lee,[3] Peng Fei,[4] Jinhyoung Park,[3] Shadi Bohlool,[3] Lian Lash-Rosenberg,[3] K. Kirk Shung,[3] and Tzung K. Hsiai[1,2]

Abstract

Myocardial infarction results in scar tissue and irreversible loss of ventricular function. Unlike humans, zebrafish has the capacity to remove scar tissue after injury. To assess ventricular function during repair, we synchronized microelectrocardiogram (μECG) signals with a high-frequency ultrasound pulsed-wave (PW) Doppler to interrogate cardiac hemodynamics. μECG signals allowed for identification of PW Doppler signals for passive (early [E]-wave velocity) and active ventricular filling (atrial [A]-wave velocity) during diastole. The A wave ($9.0 \pm 1.2\,cm \cdot s^{-1}$) is greater than the E wave ($1.1 \pm 0.4\,cm \cdot s^{-1}$), resulting in an E/A ratio <1 (0.12 ± 0.05, $n=6$). In response to cryocauterization to the ventricular epicardium, the E-wave velocity increased, accompanied by a rise in the E/A ratio at 3 days postcryocauterization (dpc) (0.55 ± 0.13, $n=6$, $p<0.001$ vs. sham). The E waves normalize toward the baseline, along with a reduction in the E/A ratio at 35 dpc (0.36 ± 0.06, $n=6$, $p<0.001$ vs. sham) and 65 dpc (0.2 ± 0.16, $n=6$, $p<0.001$ vs. sham). In zebrafish, E/A <1 at baseline is observed, suggesting the distinct two-chamber system in which the pressure gradient across the atrioventricular valve is higher compared with the ventriculobulbar valve. The initial rise and subsequent normalization of E/A ratios support recovery in the ventricular diastolic function.

Introduction

Adult mammalian ventricular cardiomyocytes have a limited capacity to regenerate from the significant loss of myocardium.[1–3] Injured human hearts heal by forming scar tissues, which lack contractile phenotype and constitute a substrate for arrhythmia and ventricular remodeling.[4] However, nonmammalian vertebrates, such as Zebrafish (*Danio rerio*), are capable of removing scar tissue during heart regeneration, thus providing a genetically tractable model in identification of barriers to sufficient cardiac regeneration in mammals.[5–7]

Despite having a two-chambered heart and lacking a pulmonary vasculature, the zebrafish heart action potential (AP) shape and electrocardiogram (ECG) patterns are remarkably similar to those of humans in P waves, QRS complexes, and T waves.[8,9] By using the microelectrodes, we previously demonstrated the dynamic changes in corrected QT (QTc) intervals in response to ventricular amputation.[10] Despite histological evidence of gap junctions such as CX43 in the regenerated cardiomyocytes, ECG repolarization (QTc intervals) remained prolonged when compared to the sham at 60 days,[10] implicating the delayed rectifier potassium current (I_{kr}).[11] Thus, micro-ECG (μECG) offers a noninvasive approach to assess electrical rhythms during cardiac repair.

High-frequency ultrasound has also provided a noninvasive approach to interrogate the intracardiac structures and hemodynamics in small animals. The high-frequency ultrasound system capable of 75 MHz B-mode imaging and 45 MHz pulsed-wave (PW) Doppler measurements, which allowed for assessing ventricular filling and diastolic flow reversal in the zebrafish heart.[12] The development of a high-frame rate duplex ultrasound linear array imaging system has further allowed for both B-mode imaging and PW Doppler measurements of the mouse heart.[13] Thus, high-frequency PW Doppler provides opportunity to assess passive filling of the ventricle (early [E]-wave velocity) and active filling during atrial systole (atrial [A]-wave velocity).

In this context, we sought to coregister surface μECG with PW Doppler signals to interrogate the ventricular diastolic

[1]Division of Cardiology, Department of Medicine, University of California, Los Angeles, Los Angeles, California.
[2]Department of Bioengineering, University of California, Los Angeles, Los Angeles, California.
[3]Department of Biomedical Engineering, University of Southern California, Los Angeles, California.
[4]Department of Mechanical Engineering, University of California, Los Angeles, Los Angeles, California.
*These authors contributed equally to this work.

function during heart regeneration. Cryocauterization to the apical region of the ventricle was used to simulate epicardial injury during myocardial infarction.[6,7] Synchronous μECG with PW Doppler signals allowed for identification of passive filling (E-wave velocity) and active filling (A-wave velocity) of the ventricle during diastole. Unlike that of human hearts, the A-wave is greater than the E wave in zebrafish, and the E/A ratio is less than 1 at baseline. Previous studies also demonstrated that the E/A ratio of neonatal mice is less than 1 and increased to about 4 as they matured.[14,15] E/A ratios increased at 3 days postcryocauterization (dpc) due to an increase in E waves. The E/A ratios and E waves gradually decreased at 35 and 65 dpc toward the baseline. PR and RR intervals remained unchanged during cardiac regeneration; however, QTc intervals remained prolonged, reminiscent of ventricular amputation.[10] These findings demonstrate that integrating μECG and PW Doppler provides a novel strategy to elucidate changes in cardiac rhythms, hemodynamics, and ventricular function during cardiac repair. Distinct from humans, the E/A ratio is <1 at the baseline level and passive filling (E wave) increased in response to injury in a two-chamber system, in which pressure gradient across the atrioventricular (AV) valve is higher compared with the ventriculobulbar (VB) valve.

Designs and Methods

Zebrafish experiments were performed in compliance with the Institutional Animal Care and Use Committees (IACUC) at the University of Southern California (USC) (IACUC with permit number 11110). Animals were euthanized for signs of suffering in compliance with the Guide for the Care and Use of Laboratory Animals of the National Institutes of Health. Adult zebrafish (>1 year old), 3–4 cm in length (Tong's Tropical Fish and Supplies), were maintained in a recirculating aquarium system (Aquaneering, Inc.) that provides a physiological environment for zebrafish habitat, including an automatic light cycle, temperature control at 28°C, and pH monitoring.

μECG acquisition

Before measurement, an open-chest procedure was performed and the silver lining layer underneath the fish skin was removed to allow for detection of μECG signals through the microneedle (AD Instrument). The sedated fish (in 0.04% Tricaine methane sulfonate—Tricaine) were first placed in a damp sponge, ventral side up, and then the open-chest surgery was carried out.[10,16] For ECG acquisition, the working electrode was positioned closely above the ventricle and between the gills, while the corresponding reference electrode was placed close to the tail.

The signals were amplified by 10,000-fold (1700 Differential Amplifier; A-M Systems, Inc.) and filtered between 0.1 and 500 Hz at a cutoff frequency of 60 Hz (notch). Wavelet transform and thresholding techniques were used to enhance signal-to-noise ratios (Matlab; MathWorks, Inc.) for the individual ECG recording, as previously reported.[16]

μECG signals were analyzed for P waves, QRS, QT, and RR intervals. QT intervals were corrected for heart rate variability due to the use of a sedative agent (Tricaine) as

$$QT_c = \frac{QT}{\sqrt{RR}} \quad [1]$$

Alternatively, we established a correlation (R^2) between QT (ms) and RR (s) by recordings of multiple zebrafish, as reported by Milan and Macrae.[17] A linear equation $\mathrm{QT} = \mathrm{QTc} \times \sqrt{\mathrm{RR\ interval}}$ was established.

PW Doppler acquisition

Blood flow velocities in the zebrafish heart were measured using a high-frequency ultrasound array imaging system[18] with a 30 MHz 256-element linear array transducer.[18] The sedated zebrafish were placed on a test bed with its ventral side facing upward. The array transducer mounted on a mechanical positioner placed above the ventral side of the zebrafish. Under the guidance of B-mode imaging, the Doppler gate (window) was positioned upstream from the AV valve and downstream from the VB valve to interrogate both inflow velocities from the atrium and outflow velocities to the aortic valves (Fig. 1C). The pulse repetition frequency for PW Doppler was set to be 9.5 kHz and the estimated Doppler angle was 0°, since the blood flow of the zebrafish cardiac chambers was in the dorsal–ventral direction. PW Doppler signals for the peak early diastolic velocity (early passive filling E wave) and the peak late diastolic velocity (active filling A wave) were recorded for the control (sham) and the cryocauterization groups for ~ 3 s and were stored for further offline analysis using Matlab.

The signal processing of the PW Doppler was based on in-phase and quadrature (IQ) demodulation and complex Fast Fourier Transform (cFFT).[19] The Doppler signals were first IQ demodulated and then low-pass filtered to remove harmonics and to reduce noise. A wall filter was also used to remove clutter signals. Doppler shift frequency was obtained by processing the IQ demodulated Doppler signals using cFFT to generate the Doppler spectrum. The Doppler shift frequency was converted to velocity using the following equation[20]:

$$v = \frac{f_d}{2f\cos\theta}c \quad [2]$$

Where f_d is the measured Doppler shift frequency, f is the center frequency of the transducer, c is the sound velocity in blood ($1540\,\mathrm{m\cdot s^{-1}}$), and θ is the angle between the ultrasound beam and the direction of the flow.

Simultaneous acquisition of ECG and PW Doppler signals

To perform ECG and PW Doppler measurements simultaneously, the sedated fish was secured on a test bed immersed in diluted tricaine (0.02%) inside a container. The aquatic environment was necessary to propagate and receive ultrasound signals at a distance, while the low concentration of tricaine helped to keep the fish sedated for 10–15 min during the experiment. The ultrasound array transducer was placed vertically above the ventral side of the fish at a distance of about 6 mm, while the two ECG electrodes were introduced laterally. The ECG electrodes were customized to give free access to the array transducer. The setup is illustrated in Figure 1A and B. A trigger signal generated from the ultrasound system was sent to the ECG recording system, and thus, we could synchronize the acquisitions. Experiments were initially performed independently to precisely locate the array transducer and the ECG electrodes, followed by simultaneous measurement.

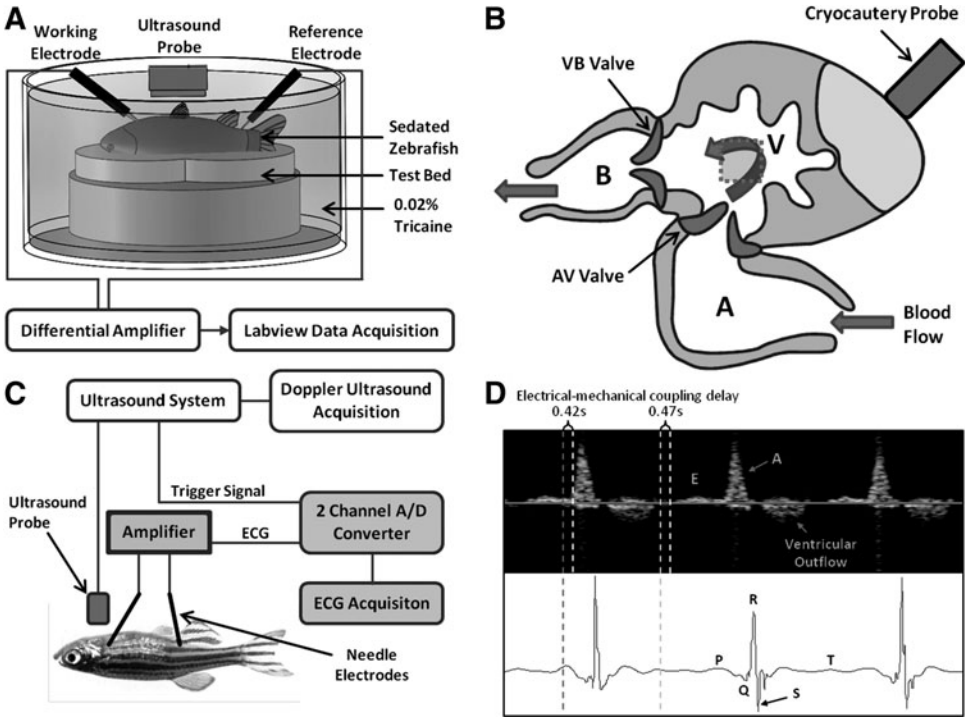

FIG. 1. Simultaneous microelectrocardiogram (μECG) and high-frequency pulsed-wave (PW) Doppler. **(A)** Relationship of microelectrodes and ultrasound probes. Adult zebrafish was sedated and placed ventral side up on a test bed filled with 0.02% Tricaine. A small opening on the chest was made to reveal the epicardial sac. Ultrasound probe was positioned at $\sim$6 mm directly above the heart. The needle electrode for ECG recording was introduced laterally to the chest and the second needle electrode was positioned to the tail as a reference. **(B)** The ultrasound system sent a trigger signal to the ECG recording system when PW Doppler recording started to synchronize both PW Doppler and ECG recordings. **(C)** The schematic diagram of the zebrafish heart illustrates ventricular apical cryocauterization by liquid nitrogen. The *gray dotted square* indicated the position of the PW Doppler gate window upstream from the atrioventricular (AV) valve and downstream from the ventricular outflow track (aortic valve). **(D)** Synchronized ECG features coregistered with the hemodynamic events as captured by PW Doppler: P wave in ECG precedes atrial contraction, resulting in A waves in Doppler; and T wave in ECG preceded ventricular relaxation, resulting in E waves in Doppler. An integration of both modalities revealed $\sim$500 ms delay in electromechanical coupling.

Cryocauterization

Cryocauterization was performed as previously described.[6] Cryocauterization-induced damage in zebrafish provides a pathophysiological model for the study of the mechanisms of scar removal postmyocardial infarction. Briefly, animals were anesthetized by immersion into 0.04% Tricaine (sigma) and immobilized by squeezing them ventral upward into a foam holder mounted on a Petri dish. A small incision was made through the body wall to open the pericardial sac. A 0.3 mm diameter copper filament (Goodfellow) linked to a polyamide tube (Parker Hanninfin) was cooled in liquid nitrogen and placed on the ventricular surface until thawing could be observed (a few seconds). Sham operations consisted of touching the exposed ventricular surface with a copper filament at room temperature. After the operation, fish were placed in a tank of fresh water, and reanimation was enhanced by pipetting water onto the gills for a couple of minutes. Fish were swimming normally after half an hour.

Ventricular inflow and outflow volumes

The ventricular active filling (A wave), passive filling (E wave), and outflow volume during a cardiac cycle were determined by multiplying the cross-sectional area (CSA) of the AV valve or VB valve by the travel distance of blood in one heartbeat (dx)

$$Volume = CSA \times dx \quad [3]$$

We assumed that CSA of two cardiac valves is circular. Since the B-mode ultrasound imaging technique could not provide a high enough resolution to clearly measure the diameter across zebrafish heart valves, valve diameters were extracted from scanning electron microscope images of adult zebrafish hearts, assuming that all of the samples have similar valve diameters.[21] The mean AV valve and VB valve diameters were 95.94 μm and 122.68 μm, respectively.

$$CSA = \pi\left(\frac{D_{valve}}{2}\right)^2 \quad [4]$$

The Doppler velocity provided the red blood cell (RBC) displacement per unit time and integrating the velocities as a function of time yielded the RBC displacement.

$$dx = \int_0^t v(t)dt \quad [5]$$

Transvalvular gradients

Based on the Doppler shift, blood flow velocities, namely, peak inflow and outflow velocities, can be converted to pressure gradients (mmHg) (ΔP) according to the Bernoulli equation.[22] Assuming that flow acceleration and viscous terms are negligible, the pressure drop across a fixed orifice can be calculated with the simplified Bernoulli equation:

$$\Delta P = \frac{1}{2}\rho\left(v_2^2 - v_1^2\right) = 4v^2 \qquad [6]$$

Where ρ denotes mass density of the blood, v_2 denotes the upstream velocity, and v_1 the downstream velocity across the valve. Furthermore, v_1 is much lower than the peak flow velocity v_2. The pressure gradient can be expressed as $4v^2$.[23] We applied Equation (6) to compare pressure gradients across AV and VB valves at baseline, 3, 35, and 65 dpc, in both sham and cryocauterization groups.

Statistical analysis

All values are expressed as mean ± SD. For statistical comparisons, we performed a two-way analysis of variance (ANOVA) followed with Tukey's method for *post hoc* analysis. p-Values < 0.05 were considered statistically significant.

Results

Synchronized surface ECG with PW Doppler signals

Synchronizing μECG with PW Doppler confirmed the A wave in response to atrial contraction (P wave) as indicated by the red dotted line and the E wave in response to passive ventricular filling by the dotted yellow line (Fig. 2). PW Doppler signals for ventricular outflow were also detected, following the QRS complex. Thus, synchronized μECG signals validated the hemodynamic events as demonstrated by PW Doppler: the P wave (atrial contraction) corresponded to the A wave; the T wave followed ventricular relaxation corresponded to the E wave; and QT intervals corresponded to ventricular outflow. A delay in electrical and mechanical coupling was observed at ~ 500 ms (Fig. 1D).

Intracardiac hemodynamics: implication of E/A ratios for diastolic function

In humans, the E-to-A ratio (E/A) is > 1 for the normal ventricular diastolic function.[23] In adult zebrafish, A-wave velocity is greater compared with the E wave (Fig. 3A, B), and the E/A ratio is < 1, suggesting a distinct cardiac physiology in the two-chamber system.[24] In response to apical injury, the E/A ratios increased due to an increase in the E wave at 3 dpc, while they remained unchanged in sham fish (Fig. 3A, C). Starting at 35 dpc, E/A ratios gradually normalized to the baseline levels.

Both active and passive filling volume and ventricular outflow track volume were derived by integrating E wave, A wave, and outflow track velocities over time, respectively (Fig. 4A–C). The ultrasound transducer was positioned to the apical region of the ventricle, and PW Doppler measured upstream from the AV valve and downstream from the VB valve (Fig. 1C). While both E and A waves exhibited positive deflection, the outflow track exhibited the negative deflection. As indicated in Equation [2], the conversion of Doppler frequency shifts to velocity is dependent on the angle of the ultrasound beam to the direction of blood flow. As the angles of inflow versus outflow profiles varied in the individual zebrafish hearts, the velocities might be underestimated. Thus, the summation of active and passive filling volumes (inflow) was greater than the outflow track volume (Fig. 4D). For example, the difference between inflow and outflow at 35 dpc was 5.3 ± 1.5 nL in the cryocauterization group and 11.2 ± 20 nL in the sham group. Nevertheless, the E/A ratios were not influenced by the angle of ultrasonic transducer and remained a reliable hemodynamic parameter for ventricular diastolic function.

We further compared pressure gradients across the AV during ventricular diastole and VB valves during ventricular systole (Fig. 5). The pressure gradient across the AV valve increased at 3 dpc and dropped over the course of regeneration,

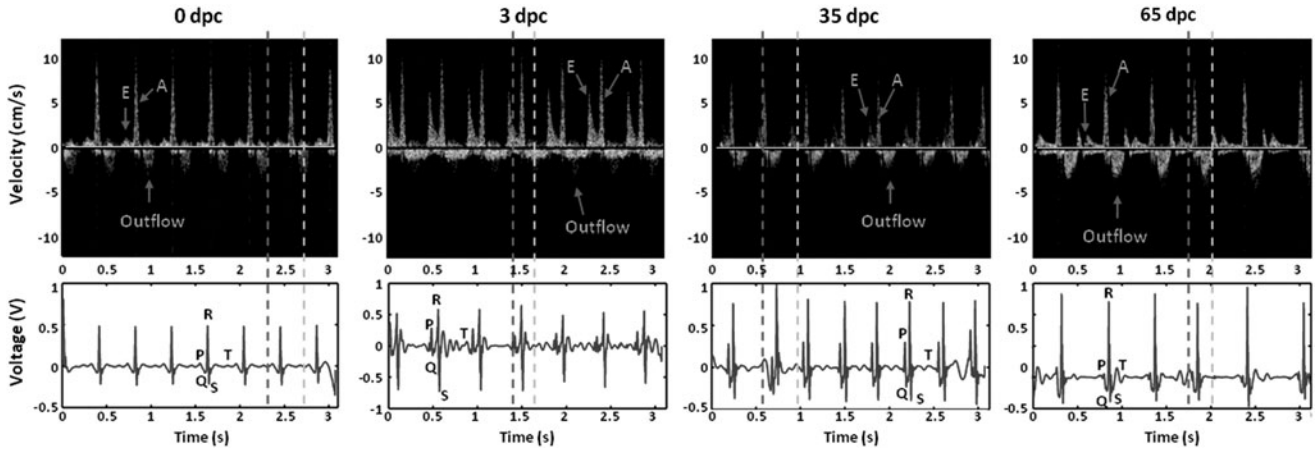

FIG. 2. Representative coregistration of PW Doppler signals with ECG signals from 0 days postcryocauterization (dpc) to 3 dpc, 35 dpc, and 65 dpc. The baseline Doppler and ECG signals were established on 0 dpc. E-wave velocity increased at 3 dpc and gradually decreased toward the baseline. In parallel, corrected QT (QTc) intervals prolonged at 3 dpc and gradually regressed to baseline levels.

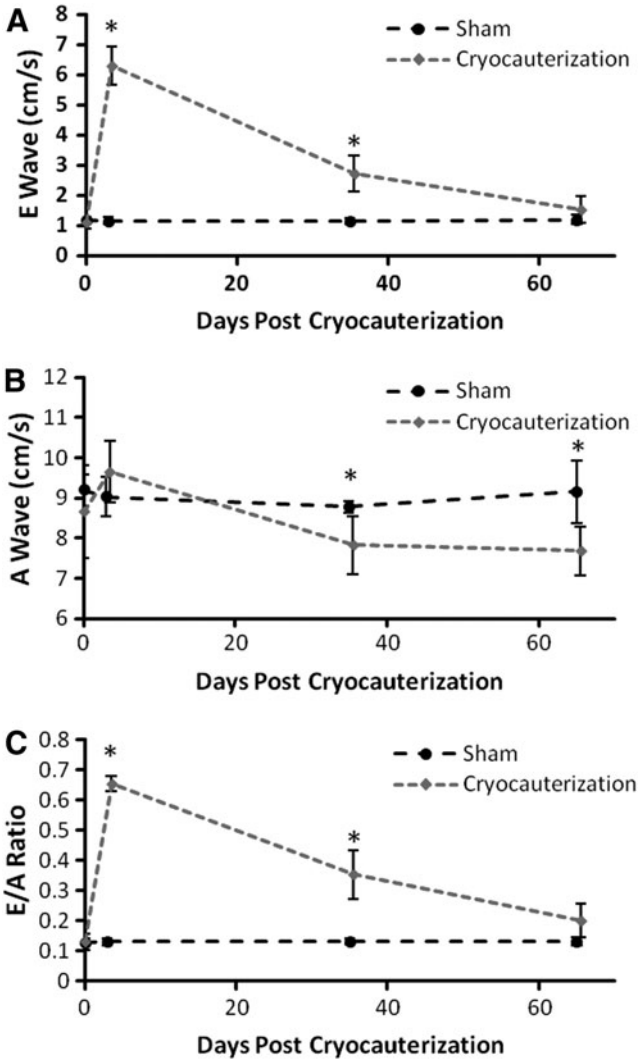

FIG. 3. Cryocauterization induced changes in mitral inflow velocities. **(A)** Cryocauterization of the zebrafish ventricle significantly increased E-wave velocities at 3 dpc, which regressed toward the baseline levels at 35 dpc ($*p < 0.001$, $n = 6$) in comparison with the sham. **(B)** A-wave velocities decreased at 35 and 65 dpc in comparison with the sham ($*p < 0.01$, $n = 6$). **(C)** Cryocauterization of the zebrafish ventricle significantly increased E/A ratios at 3 and 35 dpc ($*p < 0.001$, $n = 6$), which regressed to the baseline levels at 65 dpc. In humans, the E/A ratio is clinically assessed for ventricular compliance and it is > 1 for the normal ventricular diastolic function. In zebrafish, the E/A ratio is < 1 at baseline. The increase in the E/A ratio at 3 dpc was in parallel with the reported scarring or fibrosis, which regressed in parallel with the rapid scar regression.[6]

whereas the pressure gradient across VB valves dropped at 3 dpc and recovered at 65 dpc. Unlike humans, the range of pressure gradients across the inflow track or AV valves ($\Delta P = 1.5$–3.3 mmHg) is significantly higher compared with the outflow track or VB valves ($\Delta P = 0.3$–0.9 mmHg) in the two-chamber system. The magnitude of pressure gradients across AV by our PW Doppler was comparable to the previously reported values by a servonull pressure system.[21] Thus, the differential pressure gradients between inflow and outflow

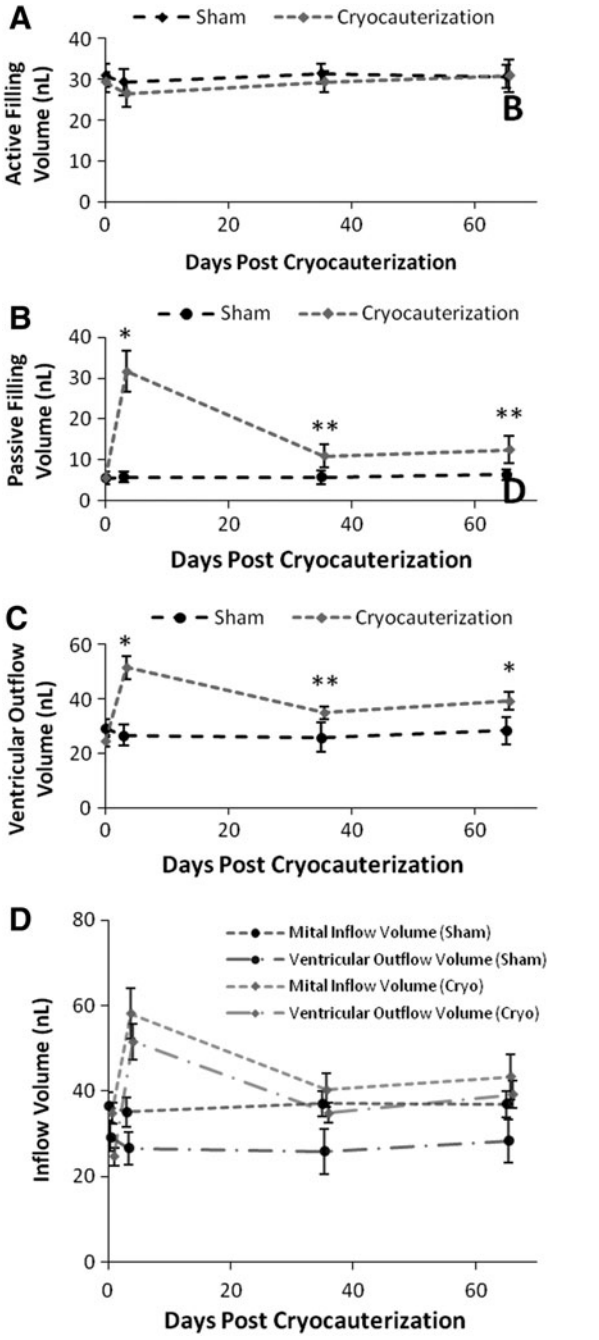

FIG. 4. Cryocauterization injury induced changes in ventricular inflow and outflow volume. **(A)** Active filling volume (A wave) remained unchanged in comparison with the sham. **(B)** Passive ventricular filling volume (E wave) was increased and remained above the baseline ($*p < 0.01$, $n = 6$). **(C)** Ventricular outflow volume was also increased above the baseline as compared to sham fish ($*p < 0.001$, $n = 6$) ($**p < 0.01$, $n = 6$). **(D)** When comparing the mitral inflow (sum of passive and active ventricular filling volume) with ventricular outflow volume, the inflow volume was measured to be larger compared with the outflow for both sham and cryoinjury. This difference was due to the angle of ultrasound beam to the direction of inflow and outflow (refer to Fig. 2C).

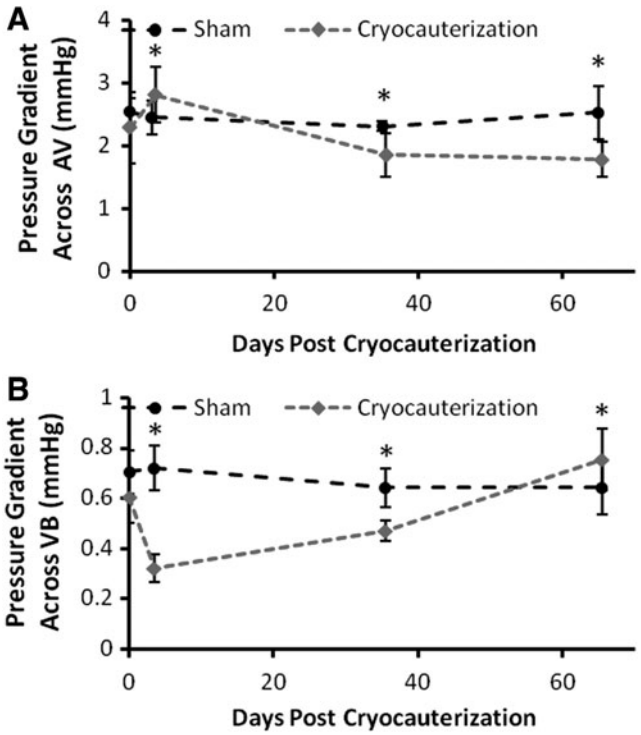

FIG. 5. Pressure gradients across AV and ventriculo-bulbar (VB) valves. **(A)** ΔP across AV valves derived from the peak velocity (A wave) increased in response to injury at 3 dpc and decreased at 35 and 65 dpc ($^*p < 0.01$, $n = 6$). **(B)** ΔP across VB valves dropped at 3 dpc and recovered at 65 dpc ($^*p < 0.001$, $n = 6$).

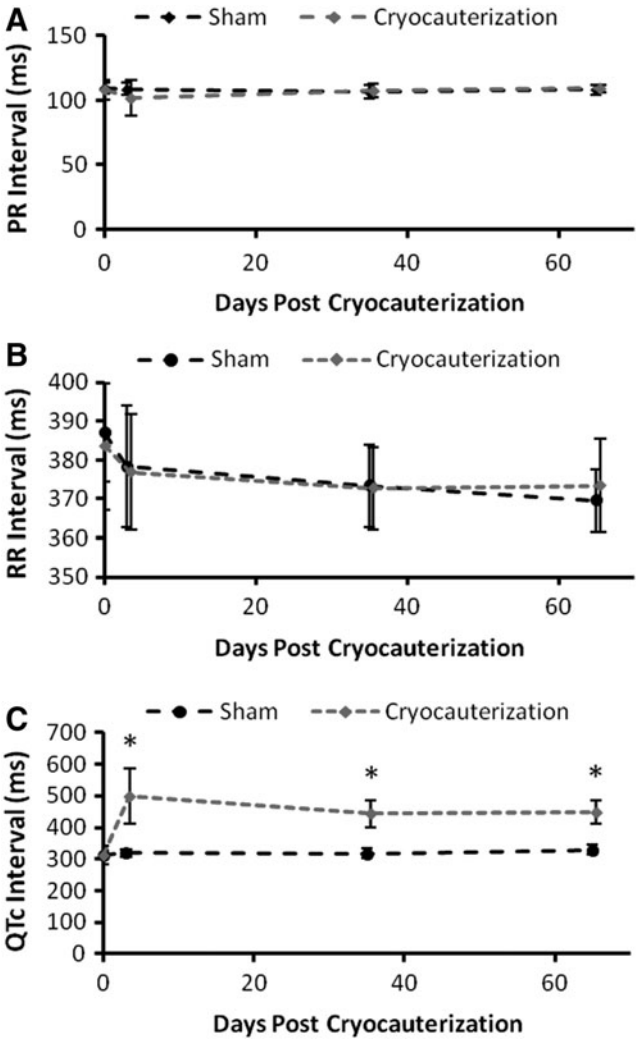

FIG. 6. Cryocauterization induced electrophysiological changes. **(A)** PR intervals and **(B)** RR intervals remained unchanged between the cryoinjury and sham groups. **(C)** The QTc intervals were prolonged in response to cryoinjury and did not recover ($^*p < 0.001$, $n = 6$), reminiscent of the same observations with ventricular amputation.

tracks further supported the distinct two-chamber physiology in association with E/A ratios < 1.

Cardiac rhythms in response to cryocauterization

Cryocauterization induced epicardial injury, simulating myocardial infarction.[6,7] While PR and RR intervals remained unchanged, the QTc intervals remained prolonged at 65 dpc. Analogous to ventricular amputation,[10] cryocauterization altered electrical repolarization phase of AP. Thus, synchronizing P waves and QT intervals with A and E waves offered a real-time and noninvasive approach to couple hemodynamics with electromechanical coupling during cardiac repair (Fig. 6).

Discussion

The novelty of our study is to elucidate hemodynamics and ventricular function in a zebrafish model of heart regeneration. Coregistration of P and T waves in μECG validated the direction and magnitude of velocity profiles across the AV valves in PW Doppler, as expressed by E/A ratios for ventricular diastolic function. Unlike humans, the E/A ratio is < 1 in zebrafish at baseline, reflecting a higher active filling (A-wave) than passive filling (E-wave) velocities during diastole in the two-chamber heart system. The dynamic changes in E/A ratios in response to injury implicated restoration of the diastolic function.

When measuring E and A waves, the ultrasound transducer was placed in parallel to the AV valve. Given the proximity and orientation of the VB valve to the AV valve, the transducer and VB valve formed a greater angle of insonation, leading to an underestimation of velocities across the VB valve. The slight variation in the transducer interrogation angle between the AV valve and VB valve led to the expected underestimation of ventricular outflow track volume, namely, the inflow volume (E wave + A wave) appeared to be greater compared with the outflow volume (Fig. 4D). However, E/A ratios were captured from the identical ultrasound angle of insonation and were not subjected to underestimation. For this reason, the E/A ratio represents a reliable strategy to assess ventricular compliance or diastolic function.

The pressure gradients across AV valves (inflow) and VB valves (outflow) during cardiac regeneration elucidated the distinct physiology in a two-chamber system (Fig. 5). The dynamics in the pressure gradient across the AV valve were consistent with the changes in A-wave velocities (Fig. 3B).

Unlike humans, the mean outflow track gradient (mmHg) was significantly less than the inflow gradient in parallel with the E/A ratio <1 in zebrafish. The magnitude of pressure gradients ($\Delta P = 1.5$–3.3 mmHg) across AV by our noninvasive PW Doppler was in close agreement with the previously reported values by an invasive servonull pressure system (peak ventricular pressure = 2.5 mmHg and atrial pressure = 0.7 mmHg).[21]

While zebrafish has been a well-recognized vertebrate model for regenerative medicine,[5] its small size and aquatic nature poses a bioengineering challenge to interrogate cardiac hemodynamics. Our PW Doppler approach revealed that atrial contraction (A wave) generated high ventricular filling pressures to the densely trabeculated ventricle in adult zebrafish.[24] In humans, myocardial infarction results in acute loss of large numbers of cardiomyocytes from necrosis.[25] The necrotic myocardium promotes recruitment of leukocyte infiltration, resulting in the clearing of dead cells from the infarct zone and replacement of the damaged tissue with collage scar.[6] Heart remodeling ensures, leading to changes in ventricular architecture and geometry, and consequently, irreversible heart failure.[25] Unlike humans, resection of $<20\%$ zebrafish ventricle triggers regeneration of the myocardium and endocardial tissues at 60 days postinjury,[5] resulting in a functional heart.[26] The increase in the E wave or E/A ratios at 3 dpc and subsequent normalization to the baseline levels at 65 dpc seemed to be in parallel with scar regression.[6,7]

Two studies have made Doppler ultrasound observations in mouse embryos. Using a closed-abdominal approach (20 MHz transducer), Gui *et al.* measured aortic flow velocities in mouse embryos from days 10 to 19.[15] Using an open-abdominal approach, Keller *et al.* monitored both dimensions and flow in 10.5–14.5-day embryos. Embryonic C57BL/6J mice have E/A ratios of 0.4 and 0.43 at 15 and 19 days postcoitum, respectively.[27] Zhou *et al.* also reported that neonatal mice also have E/A <1. The dense trabecular network in both adult zebrafish and neonatal hearts may be implicated in the E/A ratios <1. However, the E/A ratios increase as the neonates mature.[14]

Myocardial injury triggers the reactivation of epicardial marker genes.[28] In the case of zebrafish, this reactivation also occurs as a response to changes in pericardial fluid osmolality.[29] The epicardial reporter zebrafish line was used to recapitulate the expression of an endogenous epicardial marker gene in the cauterized hearts.[6] At early time points after injury, the epicardium exhibits a systemic response to injury for greater than 3 months.[6] An upregulation of epicardial genes and a massive epicardial proliferation might indicate a need to cover the damaged area.[6] In response to cryocauterization, massive expansion of the epicardial layer increased proliferation from the usual single-cell layer to a multilayer of epicardial sheets.[6] The regenerated area ballooned outward, engendering a rounder morphology (Supplementary Fig. S1; Supplementary Data are available online at www.liebertpub.com/zeb). These shape differences implicated an association with the altered ventricular diastolic function as observed by the dynamic changes in E/A ratios.[6] However, the precise mechanisms underlying rapid scar regression and normalization of E/A ratios remain to be investigated.

Assessing the T wave in μECG was challenging due to mechanical interference from low-frequency components. In μECG signals, T waves remain in the low-frequency range and are usually indistinguishable with the mechanical noises from cardiac contraction and gill respiration. The coregistration of μECG with PW Doppler signals enables unequivocal identification of E and A wave signals during cardiac regenerating.[2,10,12,30] In the current study, we have applied a high-frequency ultrasound array imaging system with the use of PW Doppler, high-frequency ultrasonic array transducers (>30 MHz).[18,20] Thus, electrical and mechanical coupling can be noninvasively interrogated in real time by μECG and E/A ratios.[10,12,16]

The limitation of our current study lies in the sample size. Some animals failed to survive during the course of repeated sedation and ECG-gated PW Doppler interrogation. Furthermore, the degrees and types of ventricular injury have an impact on the relative recovery time and mortality. To minimize animal stress, we have developed the wearable and wireless microelectrode membranes for long-term monitoring of heart injury and regeneration.[31] To reproduce the precise injury sites, we have used a micromanipulator to stabilize the 0.3 mm cupper filament for precise cryocauterization.

Overall, synchronizing μECG with PW Doppler signals is synergistic to study zebrafish hemodynamics and ventricular function. The presence of T wave and P were coregistered with the PW Doppler E and A waves to assess the inflow profiles from the atrium to ventricle. In zebrafish, E/A <1 at baseline is observed, suggesting a distinct physiology in the two-chamber system, in which atrial systole generates high ventricular filling pressure in the setting of a highly trabeculated ventricle. Our integrated approach opens a new avenue to monitor hemodynamics and ventricular function with translational implication to assess small animal models of arrhythmias and cardiomyopathy.

Acknowledgments

This study was supported by National Institutes of Health: HL083015 (T.K.H., N.C.C.), HD069305 (N.C.C., T.K.H.), and P41-EB002182 (K.K.S.).

Disclosure Statement

No competing financial interests exist.

References

1. Hsieh PC, Segers VF, Davis ME, MacGillivray C, Gannon J, Molkentin JD, *et al.* Evidence from a genetic fate-mapping study that stem cells refresh adult mammalian cardiomyocytes after injury. Nat Med 2007;13:970–974.
2. Bergmann O, Bhardwaj RD, Bernard S, Zdunek S, Barnabe-Heider F, Walsh S, *et al.* Evidence for cardiomyocyte renewal in humans. Science 2009;324:98–102.
3. Bersell K, Arab S, Haring B, Kuhn B. Neuregulin1/ErbB4 signaling induces cardiomyocyte proliferation and repair of heart injury. Cell 2009;138:257–270.
4. Hahn C, Schwartz MA. The role of cellular adaptation to mechanical forces in atherosclerosis. Arterioscler Thromb Vasc Biol 2008;28:2101–2107.
5. Poss KD, Wilson LG, Keating MT. Heart regeneration in zebrafish. Science 2002;298:2188–2190.

6. González-Rosa JM, Martín V, Peralta M, Torres M, Mercader N. Extensive scar formation and regression during heart regeneration after cryoinjury in zebrafish. Development 2011;138:1663–1674.
7. Chablais F, Veit J, Rainer G, Jaźwińska A. The zebrafish heart regenerates after cryoinjury-induced myocardial infarction. BMC Dev Biol 2011;11:21.
8. Milan DJ, Jones IL, Ellinor PT, MacRae CA. *In vivo* recording of adult zebrafish electrocardiogram and assessment of drug-induced QT prolongation. Am J Physiol Heart Circ Physiol 2006;291:H269–H273.
9. Sedmera D, Reckova M, Sedmerova M, Biermann M, Volejnik J, Sarre A, *et al.* Functional and morphological evidence for a ventricular conduction system in zebrafish and Xenopus hearts. Am J Physiol Heart Circ Physiol 2003; 284:H1152–H1160.
10. Yu F, Li R, Parks E, Takabe W, Hsiai TK. Electrocardiogram signals to assess zebrafih heart regeneration: implication of long QT intervals. Ann Biomed Eng 2010;38:2346–2357.
11. Verkerk AO, Remme CA. Zebrafish: a novel research tool for cardiac (patho) electrophysiology and ion channel disorders. Front Physiol 2012;3:255.
12. Sun L, Lien CL, Xu X, Shung KK. *In vivo* cardiac imaging of adult zebrafish using high frequency ultrasound (45–75 MHz). Ultrasound Med Biol 2008;34:31–39.
13. Zhang L, Xu X, Hu C, Sun L, Yen JT, Cannata JM, *et al.* A high-frequency, high frame rate duplex ultrasound linear array imaging system for small animal imaging. IEEE Trans Ultrason Ferroelectr Freq Control 2010;57:1548–1557.
14. Zhou YQ, Foster FS, Parkes R, Adamson SL. Developmental changes in left and right ventricular diastolic filling patterns in mice. Am J Physiol Heart Circ Physiol 2003; 285:H1563–H1575.
15. Gui YH, Linask KK, Khowsathit P, Huhta JC. Doppler echocardiography of normal and abnormal embryonic mouse heart. Pediatr Res 1996;40:633–642.
16. Sun P, Zhang Y, Yu F, Parks E, Lyman A, Wu Q, *et al.* Micro-electrocardiograms to study post-ventricular amputation of zebrafish heart. Ann Biomed Eng 2009;37:890–901.
17. Milan DJ, Macrae CA. Animal models for arrhythmias. Cardiovasc Res 2005;67:426–437.
18. Hu C, Zhang L, Cannata JM, Yen J, Kirk Shung K. Development of a 64 channel ultrasonic high frequency linear array imaging system. Ultrasonics 2011;51:953–959.
19. Aydin N, Fan L, Evans DH. Quadrature-to-directional format conversion of Doppler signals using digital methods. Physiol Measure 1994;15:181–199.
20. Shung KK. Diagnostic Ultrasound: Imaging and Blood Flow Measurements. CRC Press, Boca Raton, FL, 2005.
21. Hu N, Yost HJ, Clark EB. Cardiac morphology and blood pressure in the adult zebrafish. Anat Rec 2001;264:1–12.
22. Hudspeth RT. Fundamentals of fluid mechanics. Adv Ser Ocean Eng 2006;21:53–84.
23. Oh JK, Seward JB, Tajik AJ. The Echo Manual. Lippincott Williams & Wilkins, Philadelphia, PA, 2006.
24. Grego-Bessa J, Luna-Zurita L, del Monte G, Bolós V, Melgar P, Arandilla A, *et al.* Notch signaling is essential for ventricular chamber development. Dev Cell 2007;12: 415–429.
25. Lilly LS. Braunwald's Heart Disease: A Textbook of Cardiovascular Medicine: Elsevier Health Sciences, Philadelphia, PA, 2012.
26. Kikuchi K, Holdway JE, Werdich AA, Anderson RM, Fang Y, Egnaczyk GF, *et al.* Primary contribution to zebrafish heart regeneration by gata4+ cardiomyocytes. Nature 2010; 464:601–605.
27. Keller BB, MacLennan MJ, Tinney JP, Yoshigi M. *In vivo* assessment of embryonic cardiovascular dimensions and function in day-10.5 to -14.5 mouse embryos. Circ Res 1996; 79:247–255.
28. Lepilina A, Coon AN, Kikuchi K, Holdway JE, Roberts RW, Burns CG, *et al.* A dynamic epicardial injury response supports progenitor cell activity during zebrafish heart regeneration. Cell 2006;127:607–619.
29. Wills AA, Holdway JE, Major RJ, Poss KD. Regulated addition of new myocardial and epicardial cells fosters homeostatic cardiac growth and maintenance in adult zebrafish. Development 2008;135:183–192.
30. Lien CL, Harrison MR, Tuan TL, Starnes VA. Heart repair and regeneration: recent insights from zebrafish studies. Wound Repair Regen 2012;20:638–646.
31. Cao H, Yu F, Zhao Y, Zhang X, Tai J, Lee J, *et al.* Wearable multi-channel microelectrode membranes for elucidating electrophysiological phenotypes of injured myocardium. Integr Biol 2014;6:789–795.

Address correspondence to:
Tzung K. Hsiai, MD, PhD
Department of Medicine and Bioengineering
David Geffen School of Medicine at UCLA
Henry Samueli School of Engineering & Applied Science
Los Angeles, CA 90073

E-mail: thsiai@mednet.ucla.edu